Wind and Structures, Vol. 7, No. 6 (2004) 373-392

DOI: http://dx.doi.org/10.12989/was.2004.7.6.373

Spatial extrapolation of pressure time series on low buildings using proper orthogonal decomposition

Yingzhao Chen†, Gregory A. Kopp‡ and David Surry‡†

Alan G. Davenport Wind Engineering Group, Boundary Layer Wind Tunnel Laboratory, The University of Western Ontario, London, Ontario, N6A 5B9, Canada

(Received August 6, 2003, Accepted September 3, 2004)

Abstract. This paper presents a methodology for spatial extrapolation of wind-induced pressure time series from a corner bay to roof locations on a low building away from the corner through the application of proper orthogonal decomposition (POD). The approach is based on the concept that pressure time series in the far field can be approximated as a linear combination of a series of modes and principal coordinates, where the modes are extracted from the full roof pressure field of an aerodynamically similar building and the principal coordinates are calculated from data at the leading corner bay only. The reliability of the extrapolation for uplift time series in nine bays for a cornering wind direction was examined. It is shown that POD can extrapolate reasonably accurately to bays near the leading corner, given the first three modes, but the extrapolation degrades further from the corner bay as the spatial correlations decrease.

Keywords: proper orthogonal decomposition; extrapolation; pressure time series; low-rise buildings; database-assisted design.

1. Introduction

Surface pressure fluctuations on bluff bodies (such as low buildings) have complex temporal and spatial features due to flow separation and turbulence. As a spatio-temporal description of a random field, the proper orthogonal decomposition technique (POD) provides a unique tool to represent the fluctuating pressure field. This has many practical uses related to determining structural loads for engineering analyses or the extraction of spatial and temporal features for better physical interpretations. The original idea of POD appears to be independently developed by several people including Kosambi (1943), Loève (1945), Karhunen (1946), Pougachev (1953) and Obukhov (1954), as noted by Lumley (1970). POD is also known as the Karhunen-Loève Expansion (Loève 1978) or Principal Component Analysis (Jolliffe 1986), and has been widely applied to analyze random fields for the purposes of data reduction, image compression, and feature extraction in a variety of disciplines. In fluid mechanics, POD was first introduced in the context of turbulence by Lumley (1967) to extract organized (i.e., coherent) structures of inhomogeneous turbulent flow fields. Since then, it has been successfully used to investigate coherent structures in many turbulent flows including jets, wakes, shear layers

† Post-Doctoral Fellow, Presently in the Department of Civil Engineering and Engineering Mechanics, Columbia University
‡ Associate Professor and Canada Research Chair in Environmental Fluid Mechanics
‡† Professor and Research Director

and boundary layers (e.g., Lumley 1981, Glauser, *et al*. 1987, Berkooz, *et al*. 1993). In wind engineering, the first application for the representation of pressure fluctuations is attributed to Armitt (1968). Many applications include those of Kareem and Cermak (1984), Holmes (1990), Ho (1992), Letchford and Mehta (1993), Davenport (1995), Bienkiewicz, *et al*. (1995), Tamura, *et al*. (1997, 1999), Holmes, *et al*. (1997), Jeong, *et al*. (2000), and so on. Among these examples, POD was mainly used for extracting orthogonal modes from the random field for structural load analyses.

Data reduction, interpolation and extrapolation are important issues in the use of aerodynamic databases for design of buildings. The concept of database-assisted design (DAD) would make direct use of pressure time series from aerodynamic databases to perform numerical structural analyses of wind loads on low buildings (e.g., Simiu and Stathopoulos 1997, Rigato, *et al*. 2001, Whalen, *et al*. 2002). Since no aerodynamic database could ever be complete, and designers need freedom to choose building shapes, we have been addressing many issues pertaining to the interpolation and extrapolation of pressure time series on low buildings to make DAD practically feasible. This work has been recently summarized in Kopp, *et al*. (2003), with details given in Chen, *et al*. (2002, 2003a, 2003b, 2003c).

The present work is motivated by different, but related issues. We had experimental data from a corner panel on the roof of a generic low building. These data, which included more than 700 pressure taps in a corner panel of an equivalent full-scale area of 12 ft by 25 ft (3.7 m by 7.6 m), were used in a numerical (finite element) analysis of the structural response to the roof loads (Ali and Senseny 2003). No data existed outside of the panel area and questions arose as to the boundary effects and the effects of not loading adjacent panels. Since much effort had already gone into analyzing these particular data, the idea of extrapolating the existing data to areas outside the corner panel using only the corner panel data, was examined herein. Spatial extrapolation, to our knowledge, has not been done with POD, though Delville, *et al*. (2000) use POD and linear stochastic estimation (LSE) to interface with direct numerical simulations of turbulent mixing layers. The main objective of this paper is to develop a POD-based approach for extrapolation of pressure time series from a corner bay to other bays on a generic low building.

The present work also has a secondary objective. In the literature, it is found that there is debate over whether or not to use the spatial correlation matrix with or without the mean values included to extract modes from a random pressure field in POD analysis. Both ways are mathematically valid, but have different physical interpretations (Tamura, *et al*. 1999, Chatterjee 2000). Traditionally, researchers in fluid mechanics prefer to analyze velocity fluctuations (i.e., velocity time series without inclusion of mean value components), and thus the covariance matrix is employed. In contrast, in wind engineering, many researchers (e.g., Davenport 1995, Bienkiewicz, *et al*. 1995, Ho 1992), though not all, directly decompose the random pressure field with the inclusion of mean values. With this concern, Tamura, *et al*. (1999) concluded that the covariance matrix (i.e., fluctuations only) should be used because the distortion of the mode shapes leads to incorrect understanding of the underlying features of the data and flow field. However, Ferré and Giralt (1993) pointed out that if the features of the data are not naturally orthogonal, and there is no reason to assume they are, there will be a distortion and misinterpretation of the results. It was not clear to us, a priori, how these considerations would affect reconstruction and extrapolation, so the issue is also examined in the present context.

2. Review of proper orthogonal decomposition and reconstruction

2.1. Eigenvalue problem analysis

In POD analysis, spatially deterministic modes, $\Phi(x, y)$, are extracted. These modes are "most similar" to the ensemble of a random field, on average, such that they have the largest mean-square projection on the random field (Lumley 1967). Based on this definition, maximizing the inner product (i.e., projection) between modes and surface pressure field, $C_p(x, y; t)$, in the mean-square sense, leads to the Fredholm integral eigenvalue problem (Loève 1978, Lumley 1967, Armitt 1968):

$$\iint C(x, y; x', y')\Phi(x', y')dx'dy' = \lambda\Phi(x, y) \tag{1}$$

where the kernel $C(x, y;x', y')$ is defined as the two-point (zero time lag) spatial correlation between locations (x, y) and (x', y'),

$$C(x, y;x', y') = \overline{C_p(x, y;t)C_p(x', y';t)} \tag{2}$$

λ is an eigenvalue, $\Phi(x, y)$ is the corresponding eigenvector (i.e., mode), and the integral is over the whole pressure field. The rigorous derivation of the above eigenvalue problem function can be found in Loève (1978), and is also discussed by Lumley (1967) for turbulent velocity fields, and Armitt (1968), Bienkiewicz, *et al*. (1995) and Tamura, *et al*. (1999) for pressure fields. The modes can be determined from the solution of this integral eigenvalue problem.

By performing a numeric integration with a rectangular quadrature rule (Baker 1977, Glauser, *et al*. 1987, Jeong, *et al*. 2000), Eq. (1) can be written in discrete terms as:

$$\sum_{i=1}^{N} C(x_j, y_j;x_i, y_i)\Phi(x_i, y_i)\Delta A_i = \lambda\Phi(x_j, y_j) \tag{3}$$

where $\Delta A_i = \Delta x_i \Delta y_i$ is the tributary area associated with the i^{th} tap, and N is the number of pressure time series used in the ensemble of the pressure field. By setting $j = 1, 2, ..., N$, Eq. (3) can be written in a matrix format as:

$$[\mathbf{C}^{\mathbf{nu}}]\{\mathbf{\Phi}\} = \lambda\{\mathbf{\Phi}\} \tag{4}$$

where $[\mathbf{C}^{\mathbf{nu}}] = [\mathbf{C}][\mathbf{\Delta A}]$, $[\mathbf{C}]$ is the correlation matrix, and $[\mathbf{\Delta A}]$ is a diagonal matrix, whose element ΔA_i represents the tributary area of the i^{th} tap.

For a uniform grid (the simplest case), $[\mathbf{C}^{\mathbf{nu}}]$ is a real symmetric matrix (i.e., a Hermitian matrix) since $[\mathbf{C}]$ is a real symmetric matrix and $[\mathbf{\Delta A}]$ is a scalar matrix. Hence, the eigenvalue problem function (Eq. (4)), which is defined by a Hermitian matrix, always give N numerically different real eigenvalues and N linearly independent and orthogonal eigenvectors (Kreyszig 1993). Eq. (4) can also be simplified into the equation directly defined by the correlation matrix (since $[\mathbf{\Delta A}]$ is a scalar matrix), as:

$$[\mathbf{C}]\{\mathbf{\Phi}\} = \lambda'\{\mathbf{\Phi}\} \tag{5}$$

where $\lambda' = \lambda/\Delta a$, Δa is the tributary area of each tap. However, for a non-uniform tap grid, $[\mathbf{C}^{\mathbf{nu}}]$

is not a symmetric matrix since each diagonal element ΔA_i is not the same (this indicates that Eq. (4) may not produce N numerically different real eigenvalues and orthogonal eigenvectors). Thus, $[\mathbf{C}^{\mathbf{nu}}]$ needs to be transformed into a Hermitian matrix (e.g., Glauser, *et al*. 1987, Jeong, *et al*. 2000), as

$$\begin{aligned}(\mathbf{C}^{\mathbf{nu}}) &= [\sqrt{\mathbf{\Delta A}}]^{-1}\{[\sqrt{\mathbf{\Delta A}}][\mathbf{C}][\sqrt{\mathbf{\Delta A}}]\}[\sqrt{\mathbf{\Delta A}}] \\ &= [\mathbf{T}]^{-1}[\mathbf{D}][\mathbf{T}]\end{aligned} \tag{6}$$

where $[\mathbf{T}] = [\sqrt{\mathbf{\Delta A}}]$ is an invertible diagonal matrix, and $[\mathbf{D}] = [\sqrt{\mathbf{\Delta A}}][\mathbf{C}][\sqrt{\mathbf{\Delta A}}]$ is a real symmetric matrix. This process is called a similarity transformation (Kreyszig 1993). According to the properties of similar matrices, $[\mathbf{C}^{\mathbf{nu}}]$ and $[\mathbf{D}]$ have the same characteristic polynomials and eigenvalues (which are N numerically different real values since $[\mathbf{D}]$ is Hermitian). Furthermore, the eigenvectors have the following relationship (Kreyszig 1993):

$$\begin{aligned}\{\mathbf{\Phi}\} &= [\mathbf{T}]^{-1}\{\mathbf{\Phi_D}\} \\ &= [\sqrt{\mathbf{\Delta A}}]^{-1}\{\mathbf{\Phi_D}\}\end{aligned} \tag{7}$$

$\{\mathbf{\Phi_D}\}$ can be determined by solving the following eigenvalue problem defined by the Hermitian matrix $[\mathbf{D}]$:

$$[\mathbf{D}]\{\mathbf{\Phi_D}\} = \lambda\{\mathbf{\Phi_D}\} \tag{8}$$

Then, substituting $\{\mathbf{\Phi_D}\}$ into Eq. (7), the eigenvector $\{\mathbf{\Phi}\}$ defined by $[\mathbf{C}^{\mathbf{nu}}]$ in Eq. (4) can be recovered for non-evenly distributed pressure taps.

2.2. Reconstruction of pressure field

Having determined the modes, the corresponding time-dependent principal coordinates can be calculated from the whole pressure field due to the orthogonality of the modes, as:

$$a_i(t) = \frac{\iint C_p(x, y; t)\Phi_i(x, y)dxdy}{\iint \Phi_i^2(x, y)dxdy} \tag{9}$$

By replacing the integral with a rectangular quadrature rule, this yields the numerical approximation,

$$a_i(t) = \frac{\sum_{j=1}^{N} C_p(x_j, y_j; t)\Phi_i(x_j, y_j)\Delta A_j}{\sum_{j=1}^{N} \Phi_i^2(x_j, y_j)\Delta A_j} \tag{10}$$

Thus, with the first few modes and the corresponding principal coordinates, the original pressure field can be reconstructed if the majority of the fluctuation energy is contained in the first few modes, i.e.,

$$\hat{C}_p(x, y;t) = \sum_{i=1}^{M} a_i(t)\Phi_i(x, y) \tag{11}$$

where $M < N$.

In order to evaluate the overall efficiency of the modes in representing the pressure field, the average fluctuating energy over the ensemble is defined as the total sum of the mean-square of the fluctuating pressure field as (e.g., Tamura, *et al.* 1999),

$$\iint \overline{C_p^2(x, y;t)}\,dxdy = \sum_{i=1}^{N} \overline{a_i^2(t)} = \sum_{i=1}^{N} \lambda_i \tag{12}$$

3. Extrapolation methodology

As implied by Eq. (11), pressure time series can be reconstructed as the product of the principal coordinates and the mode shapes. The proposed extrapolation technique is based on this equation, but with approximate forms for both $a_i(t)$ and $\Phi_i(x, y)$. The approximate form of the principal coordinates will be called $a_i^n(t)$ while the approximate mode shape is $\Phi_i^{ref}(x, y)$. We will discuss $a_i^n(t)$ first.

Eq. (10) shows that $a_i(t)$ for each mode i is the product of the area-weighted pressure coefficient and the eigenvector at a point, summed over all taps and normalized by the summation of the area-weighted eigenvector squared. Now, if every pressure coefficient and the magnitude of the eigenvector at the spatial (tap) locations were nearly equal, all would participate equally in the summation. However, if the spatial distributions were spatially non-uniform, one may be able to choose a subset of spatial locations (taps) and neglect the remainder without serious degradation of the results. It is well known that the latter situation is true for wind-induced pressures on low buildings, particularly for cornering winds where most of the energy is contained near the leading corner of the roof. Therefore, the approximation,

$$a_i^n(t) = \frac{\iint_{corner} C_p(x, y;t)\Phi_i^{ref}(x, y)\,dxdy}{\iint_{corner} \{\Phi_i^{ref}(x, y)\}^2\,dxdy} \tag{13}$$

or, in discretized form,

$$a_i^n(t) = \frac{\sum_{j=1}^{T} C_p(x_j, y_j;t)\Phi_i^{ref}(x_j, y_j)\Delta A_j}{\sum_{j=1}^{T} \{\Phi_i^{ref}(x_j, y_j)\}^2 \Delta A_j} \tag{14}$$

where the numerical integration is performed over a subset of taps, T, may be expected to be a reasonable approximation. Note that the normalization in the denominator of Eq. (14) is also over the same subset of tap locations.

In order to extrapolate to regions without pressure taps, approximate mode shapes need to be obtained. In order to perform such an approximation, the first few mode shapes cannot be random in the sense that they vary from building to building in an unknown manner. Rather, they must have some aerodynamic basis so that mode shapes obtained from an "aerodynamically similar" building could be used. Fortunately, for low buildings, it is known that, at least for the dominant modes, they are related to building aerodynamics (Baker 1999, Bekele 2004). Chen, *et al*. (2003a, 2003d) address the concept of aerodynamically similar buildings for the purpose of interpolation within the NIST aerodynamic database for DAD. This will be discussed further below.

Also related to the approximate mode shapes is the fact that they are to be used together with principal coordinates, $a_i^n(t)$, so that they should not be different in shape than those for the subset of taps used. In other words, the mode shape in the corner bay should be nearly the same if it is calculated using the entire roof or only the corner bay. Again, this is expected to hold for at least the first few modes that are governed by the aerodynamics.

Then, the pressure time series in an unknown far field, $\hat{C}_p(x, y; t)$, can be estimated from the existing pressure taps (subset, T) and the first few modes, M, as

$$\hat{C}_p(x, y; t) = \sum_{i=1}^{M} a_i^n(t) \Phi_i^{ref}(x, y) \tag{15}$$

In summary, the procedure is as follows. Pressure time history at a particular location is estimated as a series expansion of modes and approximate principal coordinates. The modes are determined from a "reference" building by solving the eigenvalue problem defined by Eqs. (7) and (8), while the approximate principal coordinates are calculated from Eq. (14) using the known taps in the corner panel. The predicted pressure time series can be used to calculate structural loads in a desired region, or they can be input to a structural analysis program.

4. Experimental data

One building geometry from the National Institute of Standards and Technology (NIST) aerodynamic database (Ho, *et al*. 2004) is employed to test the extrapolation methodology. The database of pressure time series was acquired from a series of 1:100 scale, gable-roofed, generic low building models in the Boundary Layer Wind Tunnel II at the University of Western Ontario. The building has a full-scale plan dimension of 125 ft (38.1 m) by 80 ft (24.4 m) with a roof slope of 1 in 12 and varying roof heights of 16, 24, 32 and 40 ft (4.9, 7.3, 9.8 and 12.2 m). The building dimensions and pressure tap layout of the roof surface are shown in Fig. 1. A total of 665 pressure taps were instrumented over the entire surface of the building with 335 non-uniformly distributed taps on the roof. Note that in the current work, a bay is defined as a full-scale area of 25 ft (7.6 m) by 40 ft (12.2 m) and that this is not the standard bay definition used by structural engineers. The bay located at the leading corner was instrumented with 120 taps.

Pressure time series were measured for four roof heights, 37 wind angles over a 180^o range at 5^o interval, and two upstream terrains using a high-speed solid state pressure scanning system. Two target upstream terrains (open country and suburban) were modeled in the wind tunnel model tests. The characteristics of the wind tunnel flow matched the Exposure C (open country) and Exposure B (suburban) described in ASCE 7-98 (2000). The simulated exposures have equivalent roughness lengths, z_0, of 0.03 m and 0.3 m, respectively, for open country and suburban terrain. The pressure

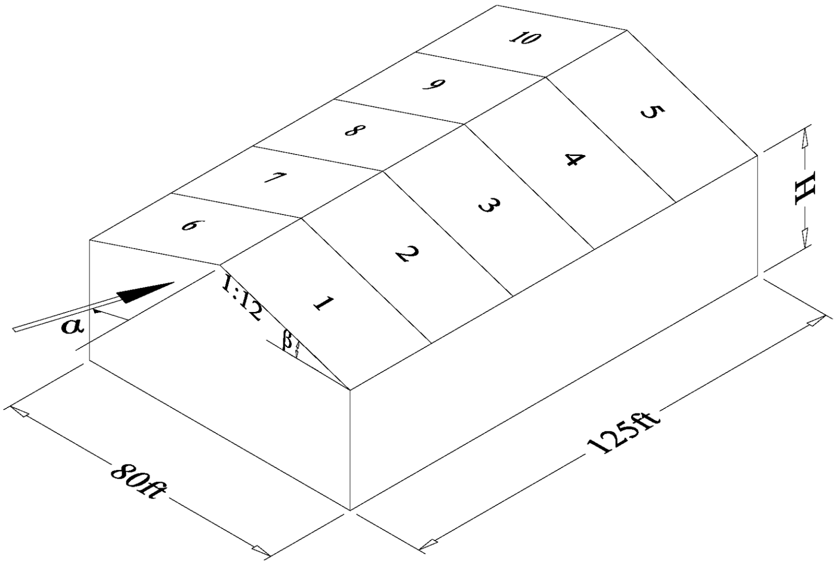

(a) The NIST building model

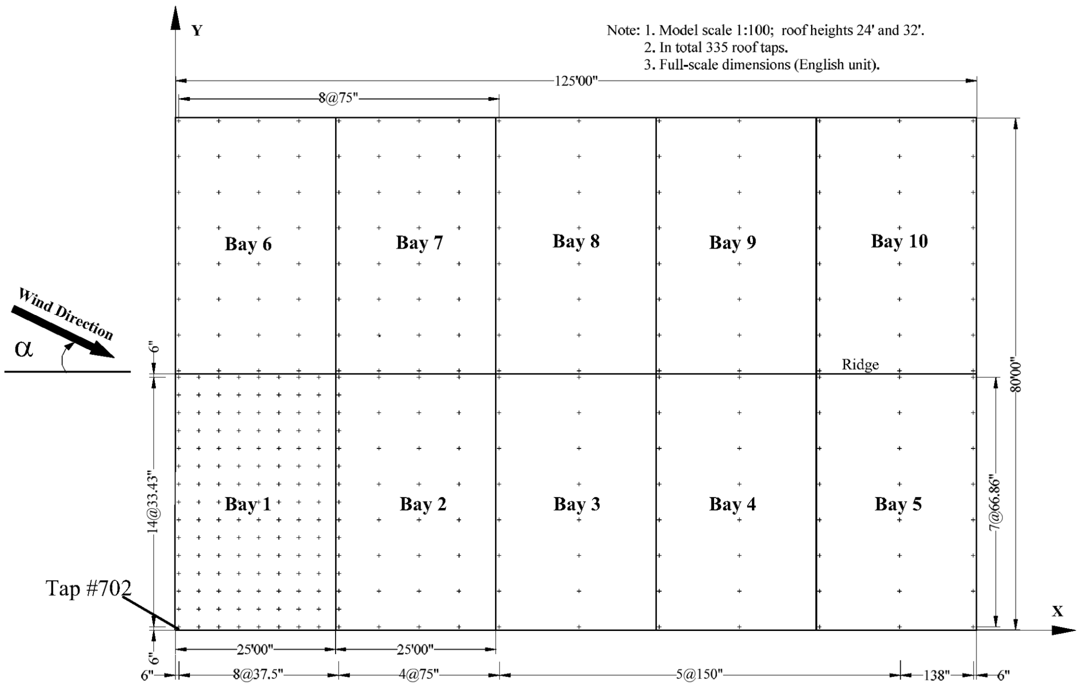

(b) Pressure tap layout of the roof surface and the definitions of bays and wind direction

Fig. 1 (a) The NIST building model, and (b) pressure tap layout of the roof surface and the definitions of bays and wind direction

signals were sampled at 500 Hz for 100 seconds and were measured essentially simultaneously. Assuming that the wind tunnel/full-scale velocity ratio is 1:3, the corresponding full-scale sampling frequency is 15 Hz. Each time series record (of 50000 data points) is then equivalent to 56 minutes in full-scale. The reference wind tunnel speed for the measurements was 45 ft/s (13.7 m/s). Typically, mean eave height speeds were about 64% of this. Pressure time series in the aerodynamic database were corrected for residual non-simultaneity and were digitally low-pass filtered at 200 Hz. All pressure coefficients used herein are referenced to the mean dynamic pressure in the uniform flow at the eaves height. A more complete description of the wind tunnel experiments can be obtained in Ho, *et al*. (2004).

In this study, the experimental data from a structurally important cornering wind direction (320^o) in open country terrain were employed in the POD analysis. The building with a roof height of 32 ft (9.8 m) is used as the reference building, from which the modes will be extracted; the building with a roof height of 24 ft (7.3 m) is used as the new building, where the far field pressure data will be extrapolated from the corner bay.

5. Results and discussion

5.1. Estimation of modes

For extraction of modes, there are two different possibilities: using the spatial correlation matrix calculated from the pressure field with or without inclusion of mean value components. Based on Eq. (1), the modes can be determined from the solution of the eigenvalue problem functions using either of them. In essence, both solutions are mathematically valid, although the estimated modes would be quite different and thus lead to different interpretation of results (Tamura, *et al*. 1999, Chatterjee 2000).

Since pressure coefficients on the roof were simultaneously acquired from 335 pressure taps, the eigenvalues and modes were obtained by solving the eigenvalue problem defined by a 335×335 correlation matrix. Table 1 shows the relative contributions from the first 10 eigenvalues computed for the surface pressure field with and without the mean values for a wind direction of 320^o. As shown by other authors (e.g., Tamura, *et al*. 1999), this leads to significantly different results. With the mean included, the proportion of the first mode to the total mean square is 91%, which is much larger than that from the covariance matrix (32.5%). This difference is caused by including the mean values in the calculation of the mean square, or “energy”, so that the first mode is dominated by the mean field when it is included in the calculation (Tamura, *et al*. 1999). However, both cases have similar eigenvalues for the following several modes, although their relative contributions differ. Figs. 2 and 3 depict the first three modes. Interestingly, there are no large differences (except right in the corner for mode 1) between the shapes and the normalized magnitudes of spatial modes from both cases. It is observed that the first and third modes are approximately symmetric about a quartering line on the roof along the incident wind direction, while the second mode is observed to be antisymmetric.

Fig. 4 depicts the distributions of the mean and standard deviation (or root-mean-square of the fluctuations, rms.) of pressure coefficient time series on the roof surface. There is a striking similarity between the first mode from the correlation matrix with the mean included (Fig. 2(a)) and the covariance matrix (Fig. 3(a)), the mean distribution (Fig. 4(a)) and the rms. distribution (Fig. 4(b)). This is clearly the explanation for the very high contribution of the first mode with the correlation matrix with the mean included (91%) where both the mean field and a significant fraction of the fluctuating field contribute at the same time. The “footprint” of the mean pressure distribution due to the corner vortices appears to be thinner than the rms. distribution which is reflected in mode 1 calculated both ways. The wider rms. distribution is reflected in modes 2 and 3,

Table 1 Comparison of the first 10 eigenvalues and contributions to the total fluctuating energy on the NIST building with a roof height of 32 ft (9.8 m) for a wind direction of 320^o in open country terrain

	Mean Included			Without Mean		
Mode	Mean square[1]	Eigenvalue (modal energy)	Accumulated Energy	Mean square	Eigenvalue (modal energy)	Accumulated Energy
1	524442.9	91.02%	91.02%	24725.8	32.53%	32.53%
2	16922.8	2.94%	93.95%	16652.4	21.91%	54.44%
3	5465.4	0.95%	94.90%	5464.3	7.19%	61.63%
4	3745.7	0.65%	95.55%	3713.6	4.89%	66.52%
5	2328.1	0.40%	95.96%	2249.0	2.96%	69.48%
6	1848.3	0.32%	96.28%	1847.2	2.43%	71.91%
7	1567.5	0.27%	96.55%	1559.0	2.05%	73.96%
8	1445.3	0.25%	96.80%	1442.1	1.90%	75.85%
9	1025.4	0.18%	96.98%	1020.7	1.34%	77.20%
10	985.8	0.17%	97.15%	974.1	1.28%	78.48%

[1]Note that the mean square here is not the standard deviation squared (or rms. squared), since the mean values are included.

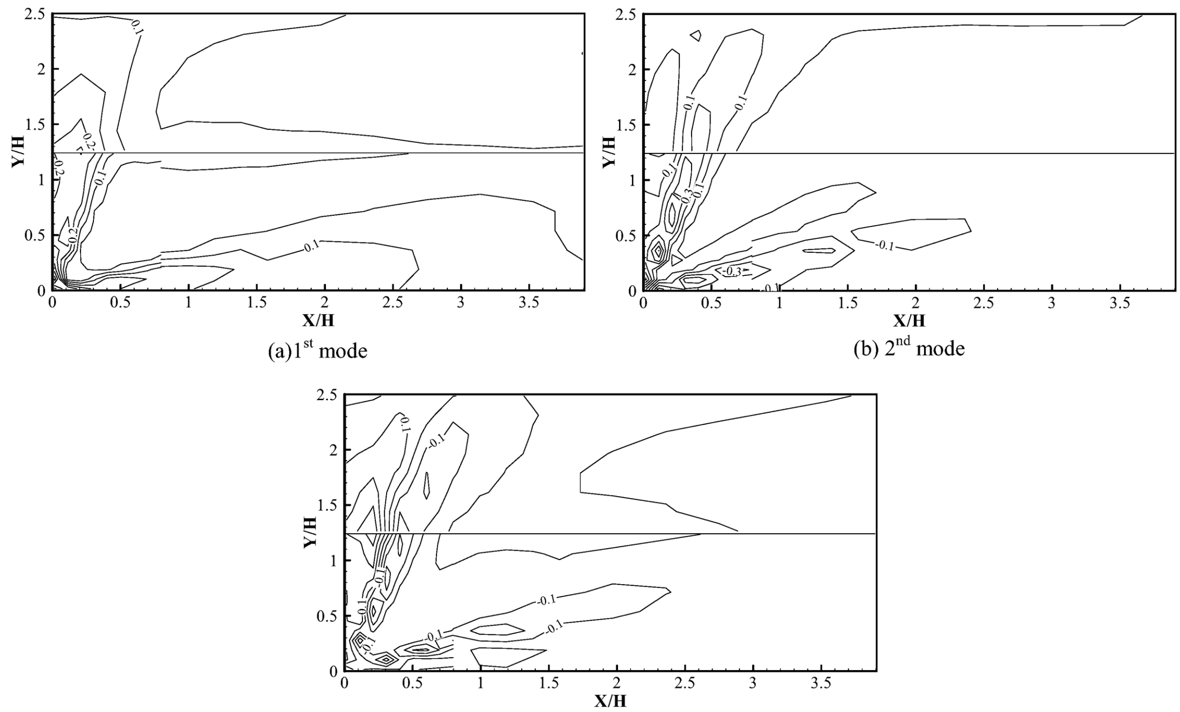

Fig. 2 Contour distributions of (a) 1st, (b) 2nd and (c) 3rd modes calculated from correlation matrix with the mean values included on the NIST building with a roof height of 32 ft (9.8 m) for a wind direction of 320^o in open country terrain

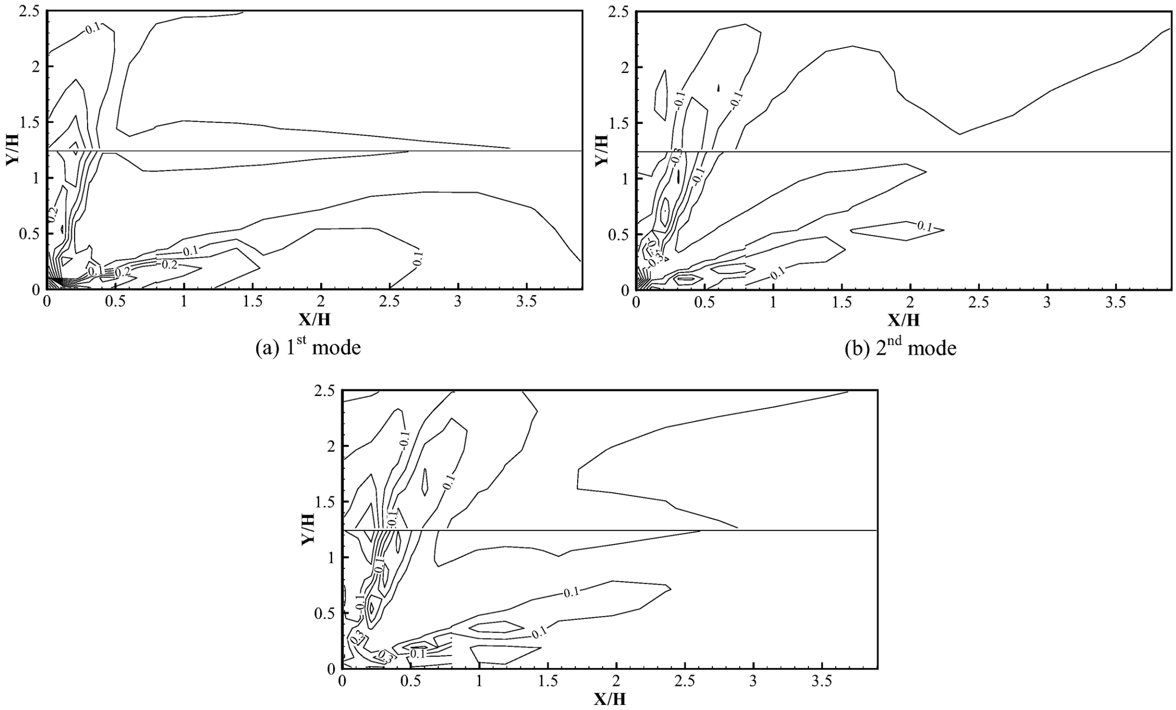

(a) 1st mode (b) 2nd mode

(c) 3rd mode

Fig. 3 Contour distributions of (a) 1st, (b) 2nd and (c) 3rd modes calculated from covariance matrix (fluctuations only) on the NIST building with a roof height of 32 ft (9.8 m) for a wind direction of 320° in open country terrain

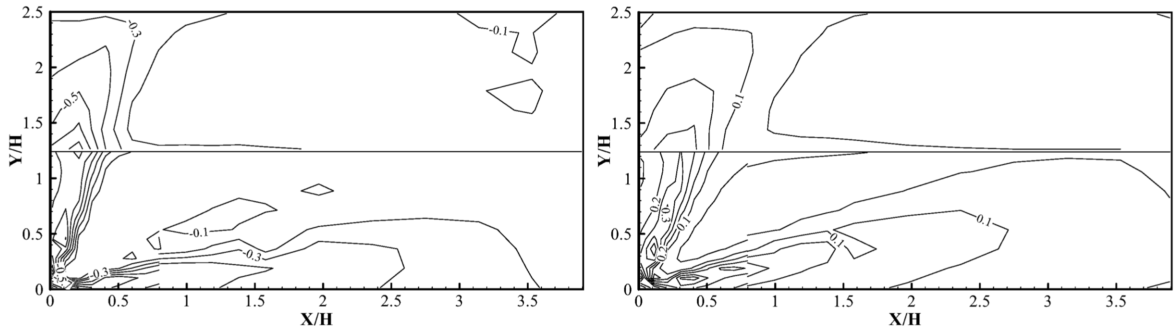

(a) (b)

Fig. 4 Contour distributions of (a) mean and (b) rms. pressure coefficients on the NIST building with a roof height of 32 ft (9.8 m) for a wind direction of 320° in open country terrain

though mode 2 being antisymmetric cannot represent the rms. by itself.

Fig. 5 depicts modes 1-3 from the covariance matrix (i.e., fluctuations only), but considering only the 120 taps in the corner bay. These are quite similar to the results presented in Fig. 3, giving some preliminary justification to the extrapolation methodology.

Geometric similarity and the use of non-dimensional groups is, of course, the cornerstone of wind

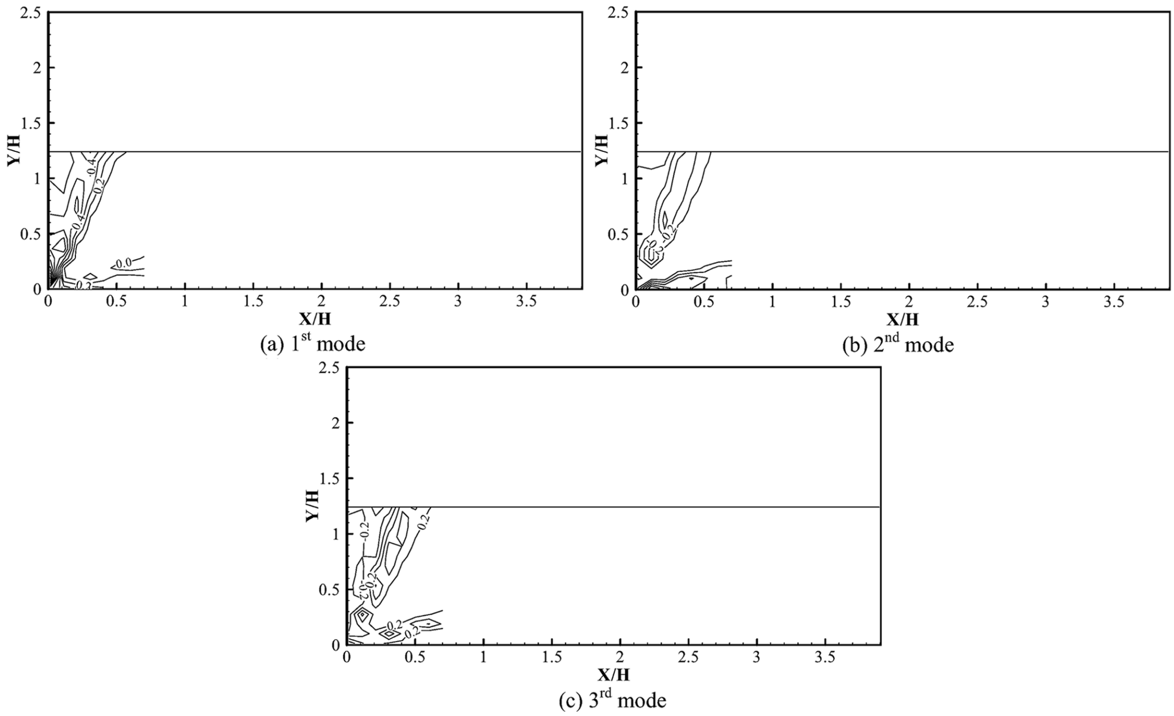

Fig. 5 Contour distributions of (a) 1st, (b) 2nd and (c) 3rd modes calculated from only the corner bay pressure field (using the covariance matrix) on the NIST building with a roof height of 32 ft (9.8 m) for a wind direction of 320° in open country terrain

tunnel testing. Chen, *et al.* (2003a, 2003d) demonstrated that true geometric and flow similarity can be relaxed for "small" perturbations and used re-scaled time series from the current 32 ft (9.8 m) high building to estimate those on the 24ft (7.3m) high building. Given their discussion, the mode shapes of the 24 ft (7.3 m) building are assumed to be close enough to use for extrapolation here. Fig. 6, which shows the first three mode shapes, indicates that they are similar to those for the 32 ft (9.8 m) building (cf., Fig. 3), again giving some preliminary justification for the extrapolation.

5.2. Reconstruction of pressure field on a reference building

This section discusses the performance of POD in reconstructing the pressure field with the first few modes by both including and excluding the mean values. This basic reconstruction is important for benchmarking how well extrapolation may possibly work. A point pressure time series of a corner tap (Tap #702) and the area-averaged uplift time series of Bays 3, 5, 6 and 10 on the NIST building with a roof height of 32 ft (9.8 m) are considered as examples (see Fig. 1 for the definitions of the corner tap and roof zones). Bays 5 and 10, which are located away from the leading corner and usually have low fluctuation energy (i.e., characterized with low rms. or mean-square values), are expected to be more difficult regions for reconstruction due to low spatial correlations between these regions.

Table 2 summarizes the reconstruction statistics of a point pressure (Tap #702) and uplift time

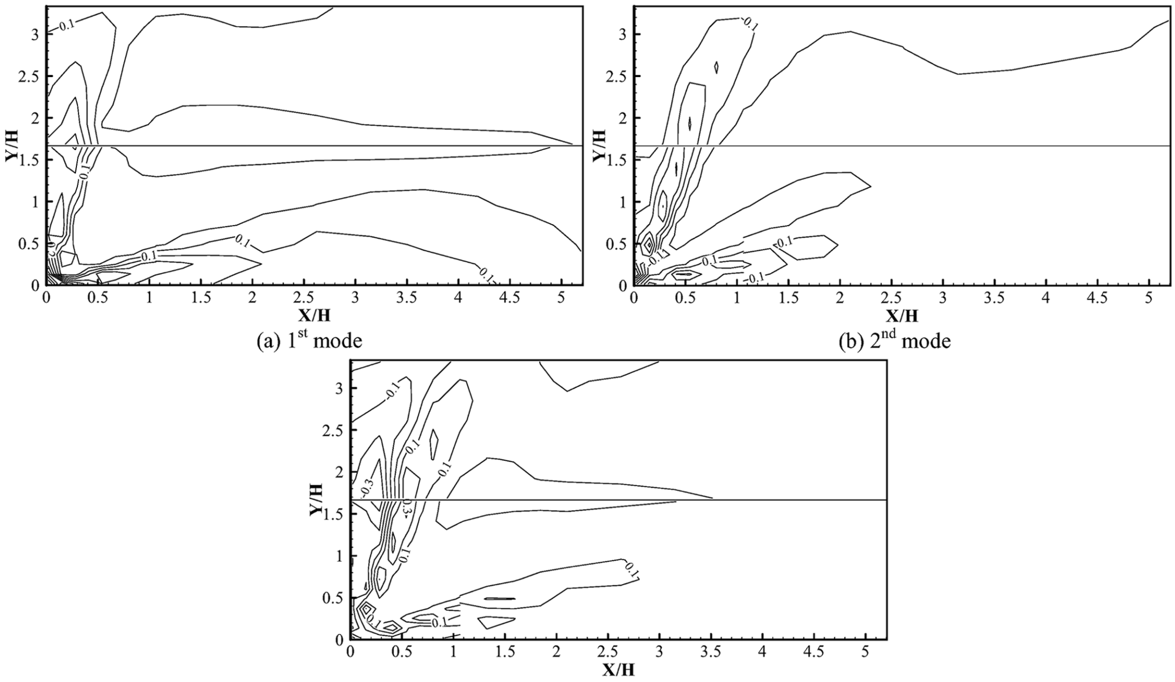

(a) 1st mode (b) 2nd mode (c) 3rd mode

Fig. 6 Contour distributions of (a) 1st, (b) 2nd and (c) 3rd modes calculated from the covariance matrix on the NIST building with a roof height of 24 ft (7.3 m) for a wind direction of 320° in open country terrain

series of Bays 3, 5, 6 and 10 for a wind direction of 320° with and without the mean included in the analysis. The comparison is at the level of basic statistics including means, rms. values, peak suctions, and correlations, while the notation POD-*i* denotes that the first *i* modes are used for the reconstruction. It is noted that the mean values are not compared in the case of using covariance matrix since the pressure fluctuations have zero means (by definition). In this case, the mean values can be reconstructed separately using other approaches, e.g., linear stochastic estimation (e.g., Chen, *et al*. 2003b) or artificial neural networks (e.g., Chen, *et al*. 2003c), but this is beyond the scope of the present study.

As shown in Table 2, in both cases, the greater the number of modes that are used, the better the reconstruction. Also, both of the methods perform better in the regions with larger fluctuation energy (i.e., larger rms.); for bays further from the leading corner, the performance is relatively poorer using only 1 or 2 modes. Not unexpectedly, it is also found that the mean value of the pressure field can be captured accurately with a maximum error of less than a few percent, given only the first mode.

Interestingly, the POD analysis including the mean values appears to exhibit similar overall performance for reconstruction of the corner pressure tap's time series and bay uplift time histories, as compared to using the covariance matrix. For some locations, it is slightly better, for others, slightly worse. For example, in Bay 6 (located in the high energy region), an excellent representation of the uplift time series can be obtained using mean values with only one mode, where the error in the reconstructed rms. is -6.4%, as opposed to the much larger error of -24% in the case of using

Table 2 Comparison of the performance of the POD analysis for reconstructing pressure time series of Tap #702 and the uplift time series of Bays 3, 5, 6 and 10 on the NIST building with a roof height 32 ft (9.8 m) for a wind direction of 320° in open country terrain. “CorrCoef ” is the correlation coefficient between the real and reconstructed fluctuations

Zone	Case	Correlation matrix with inclusion of means				Covariance matrix without inclusion of means		
		Mean	Rms.	Min.	CorrCoef	Rms.	Min.*	CorrCoef
Bay 3	Real	-0.5065	0.1468	-1.3887		0.1468	-1.3887	
	POD-1	-0.5072	0.1117	-0.9866	0.78	0.1244	-1.0855	0.85
	Error (%)	0.14%	-23.91%	-28.96%		-15.26%	-21.83%	
	POD-2	-0.5061	0.1382	-1.2053	0.93	0.1364	-1.1974	0.93
	Error (%)	-0.08%	-5.86%	-13.21%		-7.08%	-13.78%	
Bay 5	Real	-0.3996	0.1148	-0.9972		0.1148	-0.9972	
	POD-1	-0.3984	0.088	-0.7749	0.72	0.088	-0.8091	0.77
	Error (%)	-0.30%	-23.34%	-22.29%		-23.34%	-18.86%	
	POD-2	-0.398	0.1028	-0.9161	0.83	0.0949	-0.8803	0.83
	Error (%)	-0.40%	-10.45%	-8.13%		-17.33%	-11.72%	
Bay 6	Real	-0.8877	0.2079	-2.1502		0.2079	-2.1502	
	POD-1	-0.8834	0.1946	-1.7183	0.84	0.1577	-1.6216	0.76
	Error (%)	-0.48%	-6.40%	-20.09%		-24.15%	-24.58%	
	POD-2	-0.8849	0.2113	-1.8983	0.96	0.1989	-1.8589	0.96
	Error (%)	-0.32%	1.64%	-11.72%		-4.33%	-13.55%	
Bay 10	Real	-0.2719	0.0793	-0.6246		0.0793	-0.6246	
	POD-1	-0.2717	0.0599	-0.5286	0.74	0.0597	-0.5495	0.75
	Error (%)	-0.07%	-24.46%	-15.37%		-24.72%	-12.02%	
	POD-2	-0.2715	0.0623	-0.5687	0.76	0.0599	-0.5593	0.75
	Error (%)	-0.15%	-21.44%	-8.95%		-24.46%	-10.45%	
Tap#702	Real	-1.6822	0.6176	-7.5350		0.6176	-7.5350	
	POD-1	-1.682	0.3704	-3.2716	0.60	0.3438	-3.2816	0.56
	Error (%)	-0.01%	-40.03%	-56.58%		-44.33%	-56.45%	
	POD-2	-1.6846	0.3946	-3.5361	0.66	0.4081	-3.6011	0.66
	Error (%)	0.14%	-36.11%	-53.07%		-33.92%	-52.21%	

Note that to obtain the minima using the covariance matrix, the actual mean values are used.

covariance matrix. Opposite examples also occur. Fig. 7 shows autospectra of the measured and reconstructed uplift time series of Bays 5 and 6. As shown, the reconstructed autospectra are basically similar, consistent with the above comparison of statistics. Based on the above results, it can be concluded that the POD approach using only one or two modes, with or without mean values, yields reasonable results although the design-related peak values are somewhat underestimated.

5.3. Extrapolation of existing pressures to far field on a new building

Following the computational steps discussed in Section 3, pressure time series in bays adjacent to the corner bay on the NIST building with a roof height of 24 ft (7.3 m) are extrapolated with the

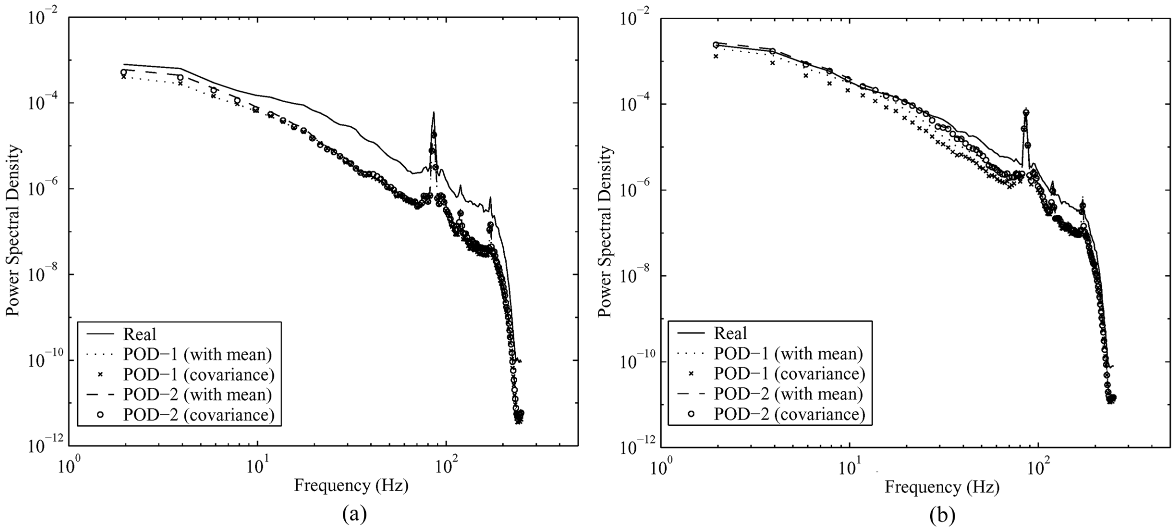

Fig. 7 Autospectra of the experimental and reconstructed uplift time series of (a) Bay 5 and (b) Bay 6 with the first and two modes on the NIST building with a roof height of 32 ft (9.8 m) for a wind direction of 320° in open country terrain

reference modes and approximate principal coordinates according to Eqs. (14)-(15), where the modes are estimated from the pressure field of the NIST building with a roof height of 32 ft (9.8 m).

5.3.1. Determination of approximate principal coordinates

The approximate principal coordinates are calculated from the pressure time series in only the leading corner bay, not the whole roof, as discussed in Section 3. Since the principal coordinate $a_i^n(t)$ is an approximation, it is necessary to compare them in order to determine how many $a_i^n(t)$ can be included for the extrapolation. This is because the errors between $a_i^n(t)$ and $a_i(t)$ may be accumulated into a much larger error if more terms are used (It is noted that this is different from the reconstruction analysis where the more modes that are used, the better the reconstruction). Thus, if $a_i^n(t)$ is in good agreement with $a_i(t)$, this should lead to good extrapolation since the POD is capable of reconstructing these pressure time series accurately with the first few modes.

The comparison between $a_i^n(t)$ and $a_i(t)$ is performed on the reference NIST building (with a roof height of 32 ft (9.8 m)). Tables 3 and 4 summarize the basic statistics for the principal coordinate time series for the first three modes obtained from the pressure field in the corner bay by including and excluding mean values, respectively. As can be seen from Table 3, it appears that only the first approximate principal coordinate, $a_1^n(t)$, can be used for the extrapolation when the mean values are included since only these statistics are close to those of the actual principal coordinates for the 32 ft (9.8 m) building. The problem is that the mean value, $\overline{a_i^n(t)}$, is significantly in error for modes 2 and 3, although the rms. is in reasonable agreement. The use of modes 2 and 3 in $a_i^n(t)$ will, therefore, not improve the extrapolation. Hence, we will use only the first mode and approximate principal coordinate time series for the extrapolation when the mean values are included.

Table 4 shows reasonable agreement in the statistics of $a_i^n(t)$ using the first three modes. Since

Table 3 Comparison of the first three real, $a_i(t)$, and approximate, $a_i^n(t)$, principal coordinates calculated using the whole roof and only the corner bay pressures, respectively, on the NIST building with a roof height 32 ft (9.8 m) for a wind direction of 320° in open country terrain

Principal Coordinates		Mean	Rms.	Min.	Max.	Skewness	Kurtosis	Correlation Coefficient
1st	$a_1(t)$	-707.2354	155.7595	-1375.6381	-173.5038	-0.42	3.11	0.89
	$a_1^n(t)$	-705.3294	184.1092	-1570.8979	-32.5661	-0.53	3.43	
	(Error %)	(-0.3%)	(18.2%)	(14.2%)	(-81.2%)	(26.2%)	(10.3%)	
2nd	$a_2(t)$	-2.0532	130.0716	-533.0464	564.3378	-0.30	3.14	0.89
	$a_2^n(t)$	-206.7174	138.9110	-936.1574	189.4330	-0.84	3.83	
	(Error %)	–	(6.8%)	(75.6%)	(-66.4%)	(180.0%)	(22.0%)	
3rd	$a_3(t)$	0.2032	73.9280	-308.3760	394.7820	0.15	3.40	0.89
	$a_3^n(t)$	-70.1026	89.5315	-410.0803	382.1785	0.42	3.93	
	(Error %)	–	(21.1%)	(33.0%)	(-3.2%)	(180.0%)	(15.6%)	

Mean values are included in the POD analysis.

Table 4 Comparison of the first three real, $a_i(t)$, and approximate, $a_i^n(t)$, principal coordinates calculated using the whole roof and only the corner bay pressures, respectively, on the NIST building with a roof height 32 ft (9.8 m) for a wind direction of 320° in open country terrain using the covariance matrix in the POD analysis

Principal Coordinates		Mean	Rms.	Min.	Max.	Skewness	Kurtosis	Correlation Coefficient
1st	$a_1(t)$	0	157.2443	-731.6159	532.7662	-0.44	3.17	0.91
	$a_1^n(t)$	0	173.4405	-793.7094	654.9665	-0.48	3.35	
	(Error %)		(10.3%)	(8.5%)	(22.9%)	(9.1%)	(5.7%)	
2nd	$a_2(t)$	0	129.0442	-477.2116	590.5984	0.6	3.42	0.91
	$a_2^n(t)$	0	136.3074	-328.2273	725.1479	0.89	3.95	
	(Error %)		(5.6%)	(-31.2%)	(22.8%)	(48.3%)	(15.5%)	
3rd	$a_3(t)$	0	73.9210	-397.5175	307.3899	-0.17	3.41	0.91
	$a_3^n(t)$	0	89.4380	-460.3844	334.3608	-0.46	3.99	
	(Error %)		(21.0%)	(15.8%)	(8.8%)	(170.6%)	(17.0%)	

$\overline{a_i^n(t)} \equiv 0$ when mean values are excluded, higher order statistics need to be checked. The rms. of $a_i^n(t)$ is reasonably accurate for the first three modes, and better than those obtained when mean values are included in the analysis. This is likely due to reduced distortion of the mode shapes when the covariance matrix is used (Tamura, *et al.* 1999). The higher order statistics also exhibit reasonable, though not perfect, agreement. Hence, for extrapolation using the covariance matrix approach, we will use the first three modes.

5.3.2. Performance in extrapolating bay uplift

Table 5 summarizes the basic statistics of the extrapolated and the actual (measured) uplift time series for Bays 2~10 for a wind direction of 320°. It can bee seen that the proposed approach is

Table 5 Statistics of the extrapolated and measured uplift time series on the NIST building with a roof height 24 ft (7.3 m) for a wind direction of 320°. "CorrCoef*" is the correlation coefficient between the reference corner bay uplift and extrapolated bay uplift time series, and "CorrCoef" is the one between the measured and extrapolated uplift time series for the same bay

Bay	Case	Mean	Rms.	Min.	CorrCoef	CorrCoef*
	Real	-0.4122	0.1385	-1.1198	1	0.67
2	POD-1 (with mean)	-0.4244	0.1166	-0.9459	0.60	0.97
	POD-3 (covariance)	–	0.1056	-0.9977*	0.87	0.87
	Real	-0.4219	0.1387	-1.1722	1	0.6
3	POD-1 (with mean)	-0.4315	0.1186	-0.9617	0.53	0.97
	POD-3 (covariance)	–	0.1008	-1.0077*	0.80	0.84
	Real	-0.4212	0.1365	-1.2639	1	0.55
4	POD-1 (with mean)	-0.4259	0.1170	-0.9493	0.50	0.97
	POD-3 (covariance)	–	0.0957	-0.9692*	0.73	0.85
	Real	-0.3432	0.1099	-0.9478	1	0.53
5	POD-1 (with mean)	-0.3389	0.0931	-0.7554	0.49	0.97
	POD-3 (covariance)	–	0.0722	-0.7398*	0.67	0.87
	Real	-0.8087	0.2006	-1.7744	1	0.88
6	POD-1 (with mean)	-0.7515	0.2065	-1.6749	0.89	0.97
	POD-3 (covariance)	–	0.2360	-2.0282*	0.89	0.93
	Real	-0.3277	0.0965	-0.8599	1	0.71
7	POD-1 (with mean)	-0.3224	0.0886	-0.7187	0.64	0.97
	POD-3 (covariance)	–	0.0811	-0.7102*	0.64	0.99
	Real	-0.2966	0.0904	-0.6809	1	0.68
8	POD-1 (with mean)	-0.2888	0.0794	-0.6437	0.63	0.97
	POD-3 (covariance)	–	0.0733	-0.6216*	0.68	0.94
	Real	-0.2428	0.0807	-0.5793	1	0.66
9	POD-1 (with mean)	-0.2410	0.0662	-0.5372	0.60	0.97
	POD-3 (covariance)	–	0.0636	-0.5175*	0.63	0.96
	Real	-0.2350	0.0793	-0.5929	1	0.61
10	POD-1 (with mean)	-0.2312	0.0635	-0.5152	0.55	0.97
	POD-3 (covariance)	–	0.0560	-0.4791*	0.61	0.96

Note that in the cases where only fluctuations are used, the minima are calculated using the actual mean values.

able to reasonably extrapolate the uplift time series near the corner bay, but appears to have increasingly larger errors further away from the reference corner both for analyses including and excluding the mean values. Several observations can be made. First, in terms of mean values, the approach is capable of accurately predicting the uplift time series in each bay with a maximum error of less than 10%. Second, in terms of rms. values and peak suctions, the peak (i.e., design) values usually underestimated (except for bay 6). The extrapolated rms. value was observed to be lower when using three modes, compared to using only one. So, since only one mode could be used when mean values were included, the rms. tends to be more accurately estimated. However, this does not necessarily translate to more accurately determined minima since, for several bays, this

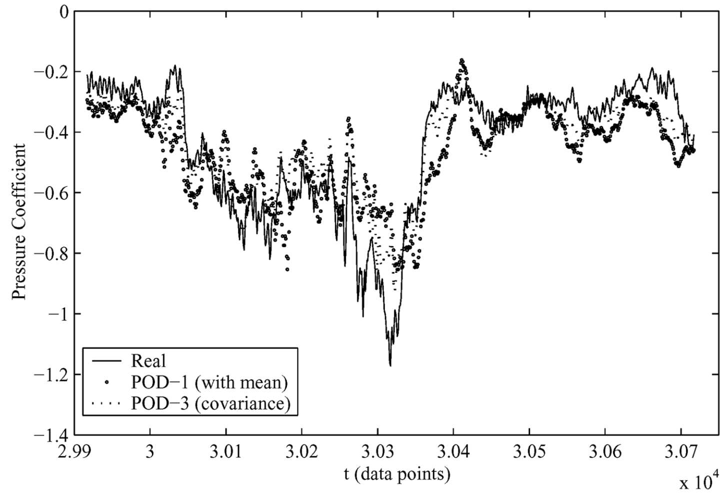

(a)

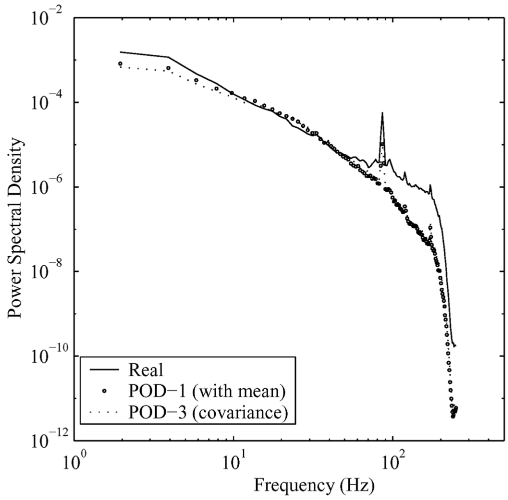

(b)

Fig. 8 (a) A short segment and (b) autospectra of Bay 3 uplift time series for the measured and POD extrapolation on the NIST building with a roof height of 24 ft (7.3 m) for a wind direction of 320° in open country terrain

statistic is more accurately determined in the analysis excluding mean values.

Third, the clear advantage of the covariance (fluctuations only) approach over that including the mean values comes when one considers the correlation between the real and extrapolated time series. The results indicate that the covariance approach using three modes "tracks" the real data much more accurately. This is indicated in two ways. First, the correlation coefficient between the real and extrapolated bay uplift time series (see CorrCoef column in Table 5) is usually higher than, and never less than, that obtained including means in the analysis. Second, the correlation coefficient between the real (reference) bay 1 uplift time series and the extrapolated (far field) bay (see CorrCoef* in Table 5) is closer to the true value (except for bay 7). When only one mode is

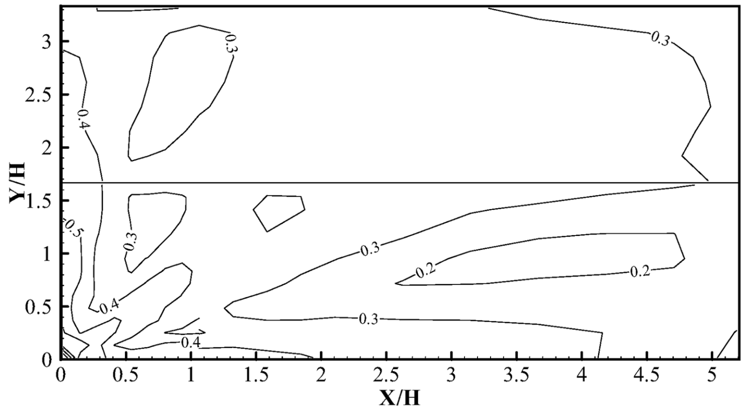

Fig. 9 Contour distribution of correlation coefficient relative to a corner Tap #702 on the NIST building with a roof height of 24 ft (7.3 m) for a wind direction of 320^o in open country terrain

used, the correlation between the extrapolated far field bays and the reference corner bay is artificially high, in fact, a value of 0.97 is maintained. Clearly, the extrapolation is following the fluctuations in the corner bay and loses the effects of turbulence in reducing this correlation. In fact, for the end bays, the true value drops to 0.53 for bay 5. When three modes are used, the spatial correlation is lower (e.g., 0.87 for bay 5), again indicating a more realistic tracking of the real data. This is the main advantage of being able to use more than one mode. Fig. 8 gives a sample of the results of the extrapolated and measured uplift time series and autospectra in Bay 3 for the wind direction of 320^o.

Fig. 9 shows the correlation coefficients relative to the corner tap #702 for a wind direction of 320^o. Clearly, the bay loads in the far field are more highly correlated with the corner bay than individual taps are with each other. This indicates that the extrapolation approach should only be used for determining structural load effects and should not be used for local loading analyses.

It should be emphasized once again that the extrapolation technique is only applicable for buildings whose correlation or covariance matrix is known, since the required modes over the whole roof are extracted from correlation or covariance matrices. In this study, the correlation matrix on an “unknown” roof is assumed to be same as that from an aerodynamically similar building. As discussed before, this assumption is reasonable only if there is small change in geometry, terrain, boundary layer characteristics, etc., so that the modes calculated accordingly will not change as well, as discussed in greater detail in Chen, *et al*. (2003a, 2003d).

6. Conclusions

A POD-based approach has been developed for extrapolation of existing wind pressure time series from a corner bay to adjacent bays on a low building roof. The technique is based on approximating both the spatial and temporal decompositions, and then combining these to estimate wind-induced pressure time series in areas on the surface of the building for which no data exist. The spatial approximation comes via the mode shapes that are used from an aerodynamically similar building, for which data exists, and which must cover the surfaces to be extrapolated. The temporal approximation comes via using a set of time series to estimate the principal coordinates that do not encompass the entire area for which the mode shapes will be used. The following conclusions can be made:

(1) There are no large differences between the distribution types and magnitudes of the first few spatial modes obtained by including or excluding mean values in the analysis. With both ways, similar accuracy in the reconstruction of the time series with the same number of modes is observed.

(2) The approach using correlation matrix with both inclusion and exclusion of mean values is able to predict the uplift time series well for regions near the (known) corner, given the first three modes and the approximated principal coordinates, but the extrapolation performance degrades further from the corner bay as the spatial correlations decrease. In the case of using covariance matrix, the mean values have to be predicted separately with other approaches, e.g., linear stochastic estimation (Chen, *et al.* 2003b) or artificial neural networks (Chen, *et al*. 2003c).

(3) Extrapolation is better when using covariance matrix since more modes can be used (three, as opposed to only one in the case of using correlation matrix with mean included). This leads to more accurate correlations between the extrapolated and actual measured data. When only one mode is used, the extrapolated time series tracks the reference data to closely, leading to artificially large spatial correlations, even though the fluctuation magnitude is underestimated. This is most likely due to the reduced distortion of the mode shapes when the covariance matrix is used (Tamura, *et al*. 1999).

Acknowledgements

The financial support of FM Global Research, and the ongoing interest of Dr. P. Senseny are gratefully acknowledged. The data were obtained under the support of the National Institute of Standards and Technology and Texas Tech University. One of the authors (GAK) acknowledges the support provided by the Canada Research Chairs Program. The authors would also like to acknowledge useful discussions with Dr. T.C.E. Ho.

References

Ali, H. and Senseny, P. (2003), "Models for standing seam roofs", *J. Wind Eng. Ind. Areod.*, **91**, 1689-1702.

Armitt, J. (1968), "Eigenvector analysis of pressure fluctuations on the West Burton instrumented cooling tower", Central Electricity Research Laboratories (U.K.), Internal Report RD/L/N, 114-168.

ASCE Standard 7-98 (2000), *Minimum Design Loads for Buildings and Other Structures, Revision of ANSI/ ASCE 7-95*, American Society of Civil Engineers, Reston, Virginia.

Baker, C.J. (1999), "Aspects of the use of the technique of orthogonal decomposition of surface pressure fields", *Wind Engineering into the 21st Century*, Larsen, Larose & Livesey (eds), Balkema, Rotterdam.

Baker, C.T.H. (1977), *The Numerical Treatment of Integral Equations*, Clarendon Press, Oxford.

Bekele, S. (2004), PhD Thesis, University of Western Ontario, London, Canada.

Berkooz, G., Holmes, P. and Lumley, J.L. (1993), "The proper orthogonal decomposition in the analysis of turbulent flows", *Annual Review Fluid Mech.*, **25**, 539-575.

Bienkiewicz, B., Tamura, Y., Ham, H.J., Ueda, H. and Hibi, K. (1995), "Proper orthogonal decomposition and reconstruction of multi-channel roof pressure", *J. Wind Eng. Ind. Aerod.*, **54**/**55**, 369-381.

Chatterjee, A. (2000), "An introduction to proper orthogonal decomposition", *Current Science*, **78**, 808-817.

Chen, Y., Kopp, G.A. and Surry, D. (2002), "Interpolation of wind-induced pressure time series with an artificial neural network", *J. Wind Eng. Ind. Aerod.*, **90**, 589-615.

Chen, Y., Kopp, G.A. and Surry, D. (2003a), "Interpolation of pressure time series in an aerodynamic database for low buildings", *J. Wind Eng. Ind. Aerod.*, **91**, 737-765.

Chen, Y., Kopp, G.A. and Surry, D. (2003b), "The use of linear stochastic estimation for the reduction of data in the NIST aerodynamic database", *Wind & Struct., An Int. J.,* **6**(2), 107-126.

Chen, Y., Kopp, G.A. and Surry, D. (2003c), "Prediction of pressure coefficients on roofs of low buildings using artificial neural networks", *J. Wind Eng. Ind. Aerod.*, **91**, 423-441.

Chen, Y., Kopp, G.A. and Surry, D. (2003d), "The NIST aerodynamic database for low buildings: some considerations for an expert system", *Proc. 11th Int. Conf. Wind Eng.*, Lubbock, Texas, 1655-1662.

Davenport, A.G. (1995), "How can we simplify and generalize wind loads?", *J. Wind Eng. Ind. Aerod.*, **54/55**, 657-669.

Delville, J., Lamballais, E. and Bonnet, J.-P. (2000), "POD, LODS, and LSE: their links to control and simulations of mixing layers", *ERCOFTAC Bulletin*, **46**, 29-38.

Ferré, J.A. and Giralt, F. (1993), "Analysis of turbulent signals", Eddy Structure Identification in Free Turbulent Shear Flows (ed. J.P. Bonnet and M.N. Glauser), Kluwer, 181-194.

Glauser, M.N., Leib, S.J. and George, W.K. (1987), *Coherent Structures in the Axisymmetric Turbulent Jet Mixing Layer*, In: Durst, F., Launder, B.E., Lumley, J.L., Schmidt, F.W. and Whitelaw, J.H. (Eds.), Turbulent Shear Flows 5 (selected papers from the fifth international symposium on the turbulent shear lows, Cornel University, 1985), 134-145, Springer-Verlag Inc.

Ho, T.C.E. (1992), *Variability of Low Building Wind Loads*, Ph.D Thesis, Department of Civil and Environmental Engineering, The University of Western Ontario, London, Canada.

Ho, T.C.E., Surry, D., Morrish D. and Kopp, G.A. (2004), "The UWO contribution to the NIST aerodynamic database for wind loads on low buildings: Part 1. Archiving format and basic aerodynamic data", *J. Wind Eng. Ind. Aerod.*, in press.

Holmes, J.D. (1990), "Analysis and synthesis of pressure fluctuations on bluff bodies using eigenvectors", *J. Wind Eng. Ind. Aerod.*, **33**, 219-230.

Holmes, J.D., Sankaran, R., Kwok, K.C.S. and Syme, M.J. (1997), "Eigenvector modes of fluctuating pressures on low-rise building modes", *J. Wind Eng. Ind. Aerod.*, **69-71**, 697-707.

Jeong, S.-H., Bienkiewicz, B. and Ham, H.-J. (2000), "Proper orthogonal decomposition of building wind pressure specified at non-uniformly distributed pressure taps", *J. Wind Eng. Ind. Aerod.*, **87**, 1-14.

Jolliffe, I.T. (1986), *Principal Component Analysis*, New York, Springer Verlag Inc., New York.

Kareem, A. and Cermak, J.E. (1984), "Pressure fluctuations on a square building model in boundary-layer flows", *J. Wind Eng. Ind. Aerod.*, **16**, 17-41.

Kopp, G.A., Chen, Y. and Surry, D. (2003), "The NIST aerodynamic database for wind loads on low buildings: an expert system to expand the database", *Proc. 2003 ASCE/SEI Structures Congress and Exposition*, Seattle (CD-ROM).

Kreyszig, E. (1993), *Advanced Engineering Mathematics* (7th Edn.), John Wiley & Sons, Inc.

Letchford, C.W. and Mehta, K.C. (1993), "The distribution and correlation of fluctuating pressures on the Texas Tech Building", *J. Wind Eng. Ind. Aerod.*, **50**, 225-234.

Loève, M. (1978), *Probability Theory II* (4th Edn.), Springer-Verlag.

Lumley, J.L. (1967), *The Structure of Inhomogeneous Turbulent Flows*, In: Yaglom, A.Y. and Tatarsky, V.I. (Eds.), Atmospheric Turbulence and Radio Wave Propagation, Nauka, Moscow, 166-178.

Lumley, J.L. (1970), *Stochastic Tools in Turbulence*, New York, Academic Press.

Lumley, J.L. (1981), "Coherent structures in turbulence", *Transition and Turbulence*, 215-242.

Rigato, A., Chang, P. and Simiu, E. (2001), "Database-assisted design, standardization and wind direction effects", *J. Struct. Eng.*, **127**, 855-860.

Simiu, E. and Stathopoulos, T. (1997), "Codification of wind loads on buildings using bluff body aerodynamics and climatological data base", *J. Wind Eng. Ind. Aerod.*, **69-71**, 497-506.

Tamura, Y., Suganuma, S., Kikuchi, H. and Hibi, K. (1999), "Proper orthogonal decomposition of random wind pressure field", *J. Fluids & Struc.*, **13**, 1069-1095.

Tamura, Y., Ueda, H., Kikuchi, H., Hibi, K., Suganuma, S. and Bienkiewicz, B. (1997), "Proper orthogonal decomposition study of approach wind-building pressure correlation", *J. Wind Eng. Ind. Aerod.*, **72**, 421-431.

Whalen, T., Sadek, F. and Simiu, E. (2002), "Database-assisted design for wind: basic concepts and software development", *J. Wind Eng. Ind. Aerod.*, **90**, 1349-1368.

AK